Journal of Hazardous Materials 178 (2010) 249–257

Contents lists available at ScienceDirect

Journal of Hazardous Materials

journal homepage: www.elsevier.com/locate/jhazmat

Parameters optimization of rice husk ash (RHA)/CaO/CeO_2 sorbent for predicting SO_2/NO sorption capacity using response surface and neural network models

Irvan Dahlan[a], Zainal Ahmad[b], Muhammad Fadly[c], Keat Teong Lee[b], Azlina Harun Kamaruddin[b], Abdul Rahman Mohamed[b,*]

[a] School of Civil Engineering, Universiti Sains Malaysia, Engineering Campus, Seri Ampangan, 14300 Nibong Tebal, Pulau Pinang, Malaysia
[b] School of Chemical Engineering, Universiti Sains Malaysia, Engineering Campus, Seri Ampangan, 14300 Nibong Tebal, Pulau Pinang, Malaysia
[c] Instrumentation and Control, Laboratory, Department of Refrigeration and Air Conditioning, Polytechnic State of Bandung, Jl. Gegerkalong Hilir, Ds. Ciwaruga Kotak Pos 1234 Bandung 40012, Indonesia

ARTICLE INFO

Article history:
Received 28 August 2009
Received in revised form 11 January 2010
Accepted 12 January 2010
Available online 18 January 2010

Keywords:
Sorbent
Rice husk ash
Air pollution
RSM model
NN model

ABSTRACT

In this work, the application of response surface and neural network models in predicting and optimizing the preparation variables of RHA/CaO/CeO_2 sorbent towards SO_2/NO sorption capacity was investigated. The sorbents were prepared according to central composite design (CCD) with four independent variables (*i.e.* hydration period, RHA/CaO ratio, CeO_2 loading and the use of RHA_{raw} or pretreated $RHA_{600°C}$ as the starting material). Among all the variables studied, the amount of CeO_2 loading had the largest effect. The response surface models developed from CCD was effective in providing a highly accurate prediction for SO_2 and NO sorption capacities within the range of the sorbent preparation variables studied. The prediction of CCD experiment was verified by neural network models which gave almost similar results to those determined by response surface models. The response surface models together with neural network models were then successfully used to locate and validate the optimum hydration process variables for maximizing the SO_2/NO sorption capacities. Through this optimization process, it was found that maximum SO_2 and NO sorption capacities of 44.34 and 3.51 mg/g, respectively could be obtained by using RHA/CaO/CeO_2 sorbents prepared from RHA_{raw} with hydration period of 12 h, RHA/CaO ratio of 2.33 and CeO_2 loading of 8.95%.

1. Introduction

Among the several air pollutants that contaminate our planet, SO_x and NO_x have received special attention due to the fact that these two pollutants have toxic and acidic characteristics. SO_x and NO_x, which are mainly resulted from the combustion of fossil/solid fuels, have been linked to the formation of acid rain and many other undesirable environmental hazards [1]. In general, SO_x and NO_x in flue gases consists of more than 98% of sulfur dioxide (SO_2) [2] and more than 90% of nitric oxide (NO) [3]. Most of the researchers are still focused on the removal of SO_2 and NO separately. Only in the last two decades, many processes have been developed for combined removal SO_2/NO technology in a complete single process which has the potential to reduce the cost of environmental pollution control technology.

Unfortunately, only limited study on the simultaneous removal of SO_2 and NO using dry method were reported at low temperature. In particular, the use of sorbent prepared from agricultural waste-derived siliceous materials, such as rice husk ash (RHA) is also scarcely reported. RHA is produced from the burning of rice husk, which is abundantly available through the rice milling process in rice-producing countries like China, India and Malaysia. In Malaysia alone, it is estimated that more than 80 thousand tones of RHA is produced annually [4,5]. Previously, we have reported the sorption characteristics of SO_2 over RHA/CaO sorbents [6–9]. It was found that the RHA/CaO ratio, type of RHA, amount of additive and hydration period used in the preparation step significantly influenced the SO_2 sorption capacity of the RHA/CaO sorbent. It was also found that this RHA/CaO sorbent was unable to remove NO gases. The simultaneous removal of SO_2 and NO can only be obtained by impregnating RHA/CaO sorbent with various metal oxides and the RHA/CaO sorbent incorporated with cerium dioxide (CeO_2) displayed the highest SO_2/NO sorption capacities [10].

Despite several reports on the simultaneous SO_2 and NO removal using dry method and the effect of sorbent preparation variables on the sorbent sorption capacity, there are no studies reported in the literature on the parameters optimization of this kind of processes. Higher sorption capacity of the sorbent can only be obtained, if all parameters are optimized. Recently, a number of statistical experimental designs with response surface methodol-

* Corresponding author. Tel.: +60 4 5996410; fax: +60 4 5941013.
E-mail address: chrahman@eng.usm.my (A.R. Mohamed).

0304-3894/$ – see front matter © 2010 Elsevier B.V. All rights reserved.
doi:10.1016/j.jhazmat.2010.01.070

Table 1
Design matrix of the four variables with the experimental and predicted values of sorbent sorption capacity.

Sample code	Hydration process variables (actual value; coded value; normalized value)				y_S (mg/g)		y_N (mg/g)	
	x_1	x_2	x_3	x_4	Exp.[a]	Predicted	Exp.[a]	Predicted
D1	12; −1; 0.25	1.5; −1; 0.25	5; −1; 0.25	RHA_{raw}; −1; 0	28.31 (0.22)	27.67	2.91 (0.67)	2.43
D2	12; −1; 0.25	1.5; −1; 0.25	15; 1; 0.75	RHA_{raw}; −1; 0	53.19 (0.85)	53.08	3.72 (0.85)	3.84
D3	12; −1; 0.25	3.5; 1; 0.75	5; −1; 0.25	RHA_{raw}; −1; 0	25.74 (0.15)	27.56	1.76 (0.40)	1.91
D4	12; −1; 0.25	3.5; 1; 0.75	15; 1; 0.75	RHA_{raw}; −1; 0	46.33 (0.67)	47.62	3.97 (0.91)	3.99
D5	24; 1; 0.75	1.5; −1; 0.25	5; −1; 0.25	RHA_{raw}; −1; 0	41.18 (0.54)	40.27	3.01 (0.69)	2.85
D6	24; 1; 0.75	1.5; −1; 0.25	15; 1; 0.75	RHA_{raw}; −1; 0	48.05 (0.72)	51.74	4.22 (0.97)	4.25
D7	24; 1; 0.75	3.5; 1; 0.75	5; −1; 0.25	RHA_{raw}; −1; 0	44.61 (0.63)	45.52	2.96 (0.68)	2.32
D8	24; 1; 0.75	3.5; 1; 0.75	15; 1; 0.75	RHA_{raw}; −1; 0	49.76 (0.76)	51.64	3.97 (0.91)	4.40
D9	18; 0; 0.5	2.5; 0; 0.5	0; −2; 0	RHA_{raw}; −1; 0	19.73 (0.00)	22.27	0.00 (0.00)	0.32
D10	18; 0; 0.5	2.5; 0; 0.5	20; 2; 1	RHA_{raw}; −1; 0	54.05 (0.87)	53.80	4.37 (1.00)	3.81
D11	18; 0; 0.5	0.5; −2; 0	10; 0; 0.5	RHA_{raw}; −1; 0	32.60 (0.33)	34.28	3.21 (0.74)	3.32
D12	18; 0; 0.5	4.5; 2; 1	10; 0; 0.5	RHA_{raw}; −1; 0	34.32 (0.37)	34.07	2.96 (0.68)	2.94
D13	6; −2; 0	2.5; 0; 0.5	10; 0; 0.5	RHA_{raw}; −1; 0	42.90 (0.59)	40.23	2.91 (0.67)	3.49
D14	30; 2; 1	2.5; 0; 0.5	10; 0; 0.5	RHA_{raw}; −1; 0	59.20 (1.00)	56.86	4.22 (0.97)	4.32
D15	18; 0; 0.5	2.5; 0; 0.5	10; 0; 0.5	RHA_{raw}; −1; 0	53.19 (0.85)	51.80	3.92 (0.90)	3.90
D16	18; 0; 0.5	2.5; 0; 0.5	10; 0; 0.5	RHA_{raw}; −1; 0	52.33 (0.83)	51.80	3.87 (0.89)	3.90
D17	18; 0; 0.5	2.5; 0; 0.5	10; 0; 0.5	RHA_{raw}; −1; 0	53.19 (0.85)	51.80	3.92 (0.90)	3.90
D18	18; 0; 0.5	2.5; 0; 0.5	10; 0; 0.5	RHA_{raw}; −1; 0	53.19 (0.85)	51.80	3.87 (0.89)	3.90
D19	18; 0; 0.5	2.5; 0; 0.5	10; 0; 0.5	RHA_{raw}; −1; 0	53.19 (0.85)	51.80	3.92 (0.90)	3.90
D20	18; 0; 0.5	2.5; 0; 0.5	10; 0; 0.5	RHA_{raw}; −1; 0	52.33 (0.83)	51.80	3.92 (0.90)	3.90
D21	12; −1; 0.25	1.5; −1; 0.25	5; −1; 0.25	$RHA_{600°C}$; 1; 1	31.74 (0.30)	30.63	2.71 (0.62)	2.37
D22	12; −1; 0.25	1.5; −1; 0.25	15; 1; 0.75	$RHA_{600°C}$; 1; 1	47.19 (0.70)	49.72	3.36 (0.77)	3.36
D23	12; −1; 0.25	3.5; 1; 0.75	5; −1; 0.25	$RHA_{600°C}$; 1; 1	29.17 (0.24)	26.55	1.86 (0.43)	1.84
D24	12; −1; 0.25	3.5; 1; 0.75	15; 1; 0.75	$RHA_{600°C}$; 1; 1	41.18 (0.54)	40.28	3.42 (0.78)	3.51
D25	24; 1; 0.75	1.5; −1; 0.25	5; −1; 0.25	$RHA_{600°C}$; 1; 1	42.04 (0.57)	43.23	2.76 (0.63)	2.78
D26	24; 1; 0.75	1.5; −1; 0.25	15; 1; 0.75	$RHA_{600°C}$; 1; 1	50.62 (0.78)	48.38	3.57 (0.82)	3.77
D27	24; 1; 0.75	3.5; 1; 0.75	5; −1; 0.25	$RHA_{600°C}$; 1; 1	47.19 (0.70)	44.52	2.56 (0.59)	2.25
D28	24; 1; 0.75	3.5; 1; 0.75	15; 1; 0.75	$RHA_{600°C}$; 1; 1	43.76 (0.61)	44.30	3.97 (0.91)	3.92
D29	18; 0; 0.5	2.5; 0; 0.5	0; −2; 0	$RHA_{600°C}$; 1; 1	26.60 (0.17)	26.41	0.00 (0.00)	0.46
D30	18; 0; 0.5	2.5; 0; 0.5	20; 2; 1	$RHA_{600°C}$; 1; 1	48.05 (0.72)	45.28	3.11 (0.71)	3.12
D31	18; 0; 0.5	0.5; −2; 0	10; 0; 0.5	$RHA_{600°C}$; 1; 1	38.61 (0.48)	36.06	2.96 (0.68)	3.05
D32	18; 0; 0.5	4.5; 2; 1	10; 0; 0.5	$RHA_{600°C}$; 1; 1	27.45 (0.20)	27.91	2.61 (0.60)	2.67
D33	6; −2; 0	2.5; 0; 0.5	10; 0; 0.5	$RHA_{600°C}$; 1; 1	35.18 (0.39)	38.05	3.47 (0.79)	3.21
D34	30; 2; 1	2.5; 0; 0.5	10; 0; 0.5	$RHA_{600°C}$; 1; 1	53.19 (0.85)	54.67	3.82 (0.87)	4.04
D35	18; 0; 0.5	2.5; 0; 0.5	10; 0; 0.5	$RHA_{600°C}$; 1; 1	48.05 (0.72)	49.61	3.67 (0.84)	3.63
D36	18; 0; 0.5	2.5; 0; 0.5	10; 0; 0.5	$RHA_{600°C}$; 1; 1	48.90 (0.74)	49.61	3.67 (0.84)	3.63
D37	18; 0; 0.5	2.5; 0; 0.5	10; 0; 0.5	$RHA_{600°C}$; 1; 1	48.90 (0.74)	49.61	3.62 (0.83)	3.63
D38	18; 0; 0.5	2.5; 0; 0.5	10; 0; 0.5	$RHA_{600°C}$; 1; 1	48.05 (0.72)	49.61	3.67 (0.84)	3.63
D39	18; 0; 0.5	2.5; 0; 0.5	10; 0; 0.5	$RHA_{600°C}$; 1; 1	48.90 (0.74)	49.61	3.67 (0.84)	3.63
D40	18; 0; 0.5	2.5; 0; 0.5	10; 0; 0.5	$RHA_{600°C}$; 1; 1	48.90 (0.74)	49.61	3.67 (0.84)	3.63

[a] Data in parenthesis are normalized values: x_1 (hydration period), x_2 (RHA/CaO ratio), x_3 (CeO_2 loading), x_4 (type of RHA), y_S (SO_2 sorption capacity), y_N (NO sorption capacity).

ogy (RSM) have been employed for studying complex processes and to determine the optimum process parameters [8,11–14]. Another approach, artificial neural network (NN), which is a non-statistical method, has also been successfully applied to estimate and model chemical and biochemical processes [15–18] and as well as in the industrial flue gas purification process [19–22]. NN accomplishes its modeling capabilities through a process known as training. There are many different approaches to train the NN. Among all the training methods, backpropagation (BP) algorithm (with Levenberg–Marquardt method) is the most widely adopted due to its ability to learn complicated multi-dimensional mappings. [19,23–25]. Most of NN studies are applied by means of sufficient or large training data. One important issue in developing NNs from data obtained from statistically based experiment design is the size of the data set which usually produces limited experimental data. Unfortunately, when a small number of data is available, one cannot expect more satisfactory training of the network and cannot accurately evaluate the network performance.

Therefore in this study, RSM was applied to examine the significant preparation variables (independent variables) affecting RHA/CaO/CeO_2 sorbent sorption capacity towards SO_2/NO (dependent variables) as well as to obtain the optimized RHA/CaO/CeO_2 sorbent. Based on previous study [6–10], three numerical variables (*i.e.* hydration period, RHA/CaO ratio and CeO_2 loading) and one categorical variable (*i.e.* the use of raw RHA or pretreated RHA at 600 °C as the starting material) have been selected as the sorbent preparation variables. Apart from that, NN model was used to verify the RSM experiment in predicting and optimizing sorbent sorption capacity. In this regard, this work will demonstrate a method to develop a NN to model, predict and optimize the RHA/CaO/CeO_2 sorbent sorption capacity using limited experimental data that is distributed into training, testing and validating data.

2. Materials and methods

2.1. Preparation of RHA/CaO/CeO_2 sorbent

In this work, two types of RHA were used in the preparation of RHA-based sorbent, *i.e.* raw RHA and pretreated RHA at 600 °C, hereinafter are referred to as RHA_{raw} and $RHA_{600°C}$, respectively. The sorbents were prepared using RHA, CaO (BDH Laboratories) and $Ce(NO_3)_3{\cdot}6H_2O$ (98%, Fluka). The raw RHA was collected from Kilang Beras & Minyak Sin Guan Hup Sdn. Bhd., Nibong Tebal, Malaysia. Prior to use, the RHA was sieved to produce less than 200 μm particle size. In order to obtain $RHA_{600°C}$ from raw RHA, the latter was further combusted in a furnace (Carbolite RWF 1200) at a temperature of 600 °C for 4 h (heating rate of 5 °C/min).

Two steps sorbent preparation were used. Water hydration method [26] was used to prepared RHA/CaO sorbent based on the optimum hydration conditions reported in our previous studies

[7]. Then, pore volume impregnation method [27] was separately employed via thermal decomposition of metal nitrate to obtain RHA/CaO/CeO_2 sorbent. The sorbent obtained in powder form was then pelletized, crushed and sieved in order to achieve the required particle size (250–300 μm) for the sorption capacity/activity test towards SO_2/NO by subjecting it to simulated flue gas.

2.2. Design, statistical analysis, model fitting and optimization

Design Expert software version 6.0.6 (STAT-EASE Inc., Minneapolis, MN) was used to generate the experimental designs, statistical analysis, regression model and to optimized the sorbent preparation variables. Central composite design (CCD) with a quadratic model and $\alpha = 2$ coupled with response surface methodology (RSM) was chosen in this study [28]. The sorbent preparation variable consists of three numerical variables, *i.e.* hydration period, x_1 (6–30 h), RHA/CaO ratio, x_2 (0.5–4.5 g/g), CeO_2 loading, x_3 (0–20%), and one categorical variable, *i.e.* the use of RHA_{raw} or $RHA_{600^\circ C}$ as the starting material (x_4). A total of 40 different combinations were performed in random order according to the CCD configuration as shown in Table 1. Three replications were carried out for all design points except the center point. The resulting sorbents were tested for SO_2/NO sorption capacity and the results are also presented in Table 1. The SO_2 and NO sorption capacities of RHA/CaO/CeO_2 sorbents were represented by y_S and y_N, respectively. The data obtained were then fitted to the following second-order polynomial equation to create response surfaces.

$$y = \beta_0 + \sum_{i=1}^{n} \beta_i x_i + \sum_{i=1}^{n} \beta_{ii} x_i^2 + \sum_{i=1}^{n-1} \sum_{j=i+1}^{n} \beta_{ij} x_i x_j \quad (1)$$

where y is the predicted responses, β the offset term (regression coefficient), x the coded value of the variable, n the number of variable, i and j are the linear and quadratic coefficients, respectively. The significance of the second-order model as shown in Eq. (1) was evaluated by analysis of variance (ANOVA). The insignificant coefficient was eliminated after the F (Fisher)-test and the final model was obtained. The model was then used to optimize the sorbent sorption capacity for all the parameters studied. Additional experiments were also carried out to verify the predicted optimize conditions.

2.3. Activity test (SO_2/NO sorption study)

The activity of the sorbent towards SO_2 or NO is expressed by SO_2 or NO sorption capacity and is defined by the weight of SO_2 or NO captured from the flue gas per gram sorbent [29,30]. The schematic diagram and details of the activity study is presented elsewhere [6,12]. The sorbent (0.5 g) was dispersed on the borosilicate glass wool (0.05 g) in the center of the reactor. The simulated flue gas (150 ml/min) was normally composed of 2000 ppm SO_2, 500 ppm NO, 10% O_2, 50% H_2O and N_2 as a balance was subsequently passed through the sorbent at a reaction temperature of 87 °C. Prior to each run, the sorbent bed was humidified for 15 min by passing N_2 gas through the humidification system with 50% relative humidity. The concentration of flue gas was measured using a Portable Flue Gas Analyzer IMR 2800P before and after the sorption process. The amount of SO_2/NO captured by the sorbent was evaluated from the time the sorbent could maintain 100% removal of SO_2/NO until it shows negligible activity. Every experimental run was repeated at least three times to increase the precision of the results, and only the average value was reported throughout this study. The repeatability of the experimental data was found to be sufficiently high with relative error between repeated runs less than 5%.

2.4. Sorbent characterization

The chemical composition of raw RHA and metal loading of the RHA-based sorbent were analyzed using Rigaku RIX 3000 X-ray Fluorescence (XRF) spectrometer. The chemical composition of RHA_{raw} is 68.0% SiO_2, 2.30% K_2O, 1.20% P_2O_5, 0.71% MgO, 0.59% CaO, 0.32% SO_3, 0.32% Cl_2O, 0.16% Al_2O_3, 0.40% others and 26.0% loss on ignition (LOI). The pretreated $RHA_{600^\circ C}$ had the following composition: 89.0% SiO_2, 2.60% K_2O, 1.50% P_2O_5, 0.86% MgO, 0.68% CaO, 0.40% SO_3, 0.26% Cl_2O, 0.21% Al_2O_3, 0.29% others and 4.20% LOI. The specific surface area, total pore volume and average pore diameter of raw materials and the sorbents were determined using BET method on a Quantachrome Autosorb analyzer. X-ray diffraction (XRD) spectrum was recorded on a Siemens D5000 X-ray diffractometer to determine the phases present in the sorbent in the range of diffraction angle (2θ) 10–70° at a sweep rate of 1° min^{-1}.

2.5. Neural network

Neural network (NN) was used as an alternative method to predict the sorbent sorption capacity based on the experimental results obtained from design of experiments. This is mainly aimed to compare the prediction obtained using central composite design approach. In this study, a feedforward network with one hidden layer was used. The topology of the NN developed was designated as 4-*h*-2 (four input neurons representing the four hydration process variables, *h* hidden neurons in a single hidden layer and two output neurons representing the SO_2 and NO sorption capacities). Trial and error search method based on the smallest sum of square error (SSE) and highest coefficient of determination (R^2) was used in order to determine the optimum number of hidden neurons (*h*). SSE was used as the error function to measure the performance of the NN according to the following equation.

$$\mathrm{SSE} = \sum_{i=1} (y_{i,e} - y_{i,p})^2 \quad (2)$$

where $y_{i,e}$ represent experimental data, $y_{i,p}$ the NN prediction and i is an index of data. A series of NN topologies with a number of hidden neurons varied from 3 to 10 was constructed, trained, tested and validated using the experimental data set in Table 1. The data sets were divided into training, testing and validation subsets, each of which contains 14 samples (D1, D4, D7, . . . D40), 13 samples (D2, D5, D8, . . . D38) and 13 samples (D3, D6, D9, . . . D39), respectively. A sigmoidal transfer function was used for the hidden neurons and is given by

$$f(x) = \frac{1}{1 + e^{-x}} \quad (3)$$

The linear transfer function was used for the input and output neurons and is given by

$$f(x) = x \quad (4)$$

All NNs were trained using the backpropagation algorithm (Levenberg–Marquardt method). The primary objective of training is to minimize the error function (SSE) by searching for a set of connection weights and biases that causes the NN to produce outputs that are equal or near to target (predicted) values. Prior to training, all data was normalized in the range of 0 ($new\,x_{\min}$) to 1 ($new\,x_{\max}$) to obtain a new scale value (x_{i-n}) by the following equation

$$x_{i-n} = \frac{x_i - x_{\min}}{x_{\max} - x_{\min}} (new\,x_{\max} - new\,x_{\min}) + new\,x_{\min} \quad (5)$$

where x_i is the input/output data (data of independent and dependent variables), $x_{\max}$ and $x_{\min}$ are the maximum and minimum values of the particular variable, respectively.

In order to generate all of these NN modeling and analysis, commercial software of MATLAB version 6.5 (The Mathworks Inc.) with

Table 2
ANOVA for the regression model equation and coefficients.

Source	Sum of squares		DF	Mean of square		*F*-test		Prob > *F*	
	y_S	y_N		y_S	y_N	y_S	y_N	y_S	y_N
Model	3594.00	34.32	13	276.46	2.64	63.29 (70.01)[a]	36.76 (57.61)[a]	<0.0001[b]	<0.0001[b]
x_3	1270.30	18.93	1	1270.30	18.93	290.80 (297.11)[a]	263.51 (257.21)[a]	<0.0001[b]	<0.0001[b]
x_2	34.99	0.28	1	34.99	0.28	8.01 (8.18)[a]	3.95 (3.86)[a]	0.0089[b] (0.0081)[a]	0.0575 (0.0586)[a]
x_1	552.63	1.37	1	552.63	1.37	126.51 (129.26)[a]	19.12 (18.67)[a]	<0.0001[b]	0.0002[b] (0.0001)[a]
x_4	47.86	0.75	1	47.86	0.75	10.96 (11.19)[a]	10.43 (10.18)[a]	0.0027[b] (0.0024)[a]	0.0033[b] (0.0032)[a]
x_3^2	595.59	10.92	1	595.59	10.92	136.35 (139.30)[a]	152.03 (150.89)[a]	<0.0001[b]	<0.0001[b]
x_2^2	976.51	1.99	1	976.51	1.99	223.55 (228.40)[a]	27.78 (26.45)[a]	<0.0001[b]	<0.0001[b]
x_1^2	33.33	0.05	1	33.33	0.05	7.63 (7.79)[a]	0.75	0.0104[b] (0.0095)[a]	0.3932
x_2x_3	28.75	0.46	1	28.75	0.46	6.58 (6.73)[a]	6.40 (6.25)[a]	0.0164[b] (0.0152)[a]	0.0178[b] (0.0179)[a]
x_1x_3	194.37	0.04	1	194.37	0.04	44.50 (45.46)[a]	0.56	<0.0001[b]	0.4602
x_3x_4	80.07	0.34	1	80.07	0.34	18.33 (18.73)[a]	4.78 (4.67)[a]	0.0002[b]	0.0380 (0.0386)[a]
x_1x_2	28.75	0.16	1	28.75	0.16	6.58 (6.73) [a]	2.25	0.0164[b] (0.0152)[a]	0.1459
x_2x_4	31.49	0.01	1	31.49	0.01	7.21 (7.37)[a]	0.07	0.0125[b] (0.0114)[a]	0.7931
x_1x_4	1.86	0.15	1	1.86	0.15	0.43	2.12	0.5194	0.1569
Residual	113.58	1.87	26	4.37	0.07	–	–	–	–

[a] Value after discarding the insignificant term; DF = degree of freedom; x_1 (hydration period), x_2 (RHA/CaO ratio), x_3 (CeO_2 loading), x_4 (type of RHA), y_S (SO_2 sorption capacity), y_N (NO sorption capacity).
[b] Significant term.

neural network toolbox was used. A modified program written in this MATLAB programming language from Ahmad and Zhang [25] was implemented.

3. Results and discussion

3.1. Response surface model

The experimental results for studying the effect of hydration period (x_1), RHA/CaO ratio (x_2), CeO_2 loading (x_3) and RHA type (x_4) are presented in Table 1 along with the predicted SO_2 and NO sorption capacities. From the data presented, sorbents D14 and D9 exhibited the highest and lowest SO_2 sorption capacities at 59.2 and 19.73 mg/g, respectively. At the same time, sorbent D10 displayed the highest NO sorption capacity at 4.37 mg/g, and sorbent D9 was not able to sorb NO. Inspection of the data tabulated in Table 1 shows that the sorbent preparation variables have a significant effect on the SO_2/NO sorption capacity of the sorbent. Using multiple regression analysis, the responses (SO_2/NO sorption capacity) obtained in Table 1 was correlated with the four sorbent preparation variables using the mathematical model as shown in Eq. (1). The final predictive equation obtained for SO_2 sorption capacity (y_S) of sorbents prepared from RHA_{raw} and $RHA_{600°C}$ (symbolized by $y_{S\text{-}1}$ and $y_{S\text{-}2}$, respectively) are given in Eqs. (6) and (7) in term of actual factor, respectively. For NO sorption capacity (y_N) of the sorbents prepared from RHA_{raw} and $RHA_{600°C}$ (symbolized by $y_{N\text{-}1}$ and $y_{N\text{-}2}$, respectively), the final equations are given in Eqs. (8) and (9), respectively.

$$y_{S\text{-}1} = -42.493 + 2.110x_1 + 20.639x_2 + 7.091x_3 - 0.023x_1^2 - 4.407x_2^2 - 0.138x_3^2 + 0.223x_1x_2 - 0.116x_1x_3 - 0.268x_2x_3 \quad (6)$$

$$y_{S\text{-}2} = -33.394 + 2.110x_1 + 18.655x_2 + 6.458x_3 - 0.023x_1^2 - 4.407x_2^2 - 0.138x_3^2 + 0.223x_1x_2 - 0.116x_1x_3 - 0.268x_2x_3 \quad (7)$$

$$y_{N\text{-}1} = -0.420 + 0.035x_1 + 0.528x_2 + 0.457x_3 - 0.192x_2^2 - 0.018x_3^2 + 0.034x_2x_3 \quad (8)$$

$$y_{N\text{-}2} = -0.280 + 0.035x_1 + 0.528x_2 + 0.416x_3 - 0.192x_2^2 - 0.018x_3^2 + 0.034x_2x_3 \quad (9)$$

From the data trend shown in Table 1, it was found that SO_2 and NO sorption capacities increased with the increase in CeO_2 loading up to maximum range of 15% for both type of RHA sorbent prepared. By increasing the amount of CeO_2, more active site was formed on the RHA/CaO sorbent to react with SO_2 and NO during the sorption process. However, it was found that the increment of CeO_2 loading to 20% (outside the range) does not have much effect on the SO_2 and NO sorption capacities as compared to 15% CeO_2 loading. This can be noticed at sorbent D10 prepared from RHA_{raw} and sorbent D30 prepared from $RHA_{600°C}$. This shows that sorption capacity of the RHA/CaO sorbent could not be further improved by excessive loading of CeO_2. This might be due to the formation of excess CeO_2 that will mainly deposit on the external surface of RHA/CaO sorbent forming pure CeO_2 which has low sorption capacity [31,32]. In addition, monolayer capacity of RHA/CaO sorbent might be exceeded at higher CeO_2 loading [33], which can form CeO_2 clusters that can block small pores of the RHA/CaO sorbent. This could reduce the accessibility of SO_2/NO molecules to the active CeO_2 coated/dispersed on the RHA/CaO sorbent. To further support this result, analysis of variance (ANOVA) was carried out for each response for the second order polynomial equations and results for the linear, quadratic and interaction terms are presented in Table 2. Hydration period (x_1) was found to have significant effect, but CeO_2 loading (x_3) has the largest effect (among the individual variable studied) on both SO_2 and NO sorption capacities due to the highest *F*-value. In contrast, RHA/CaO ratio (x_2) and type of RHA (x_4) has almost similar effect, but the effect were less pronounced (not significant) for both SO_2 and NO sorption capacities. Furthermore, the interaction between hydration period (x_1) and CeO_2 loading (x_3) was found to significantly effect SO_2 sorption capacity due to relatively high *F*-value as compared to other interaction terms. Additionally, RHA/CaO ratio (x_2) and CeO_2 loading (x_3) have about the same interaction for both SO_2 and NO sorption capacities.

Based on the statistical analysis, the proposed model was adequate, possessing no significant lack of fit and with very satisfactory values of the R^2 for all the responses. The R^2 values for SO_2 sorption capacity (y_S) and NO sorption capacity (y_N) were 0.969 and 0.937, respectively, after omitting the insignificant effects. In order to verify the prediction of CCD experiment, neural network (NN)

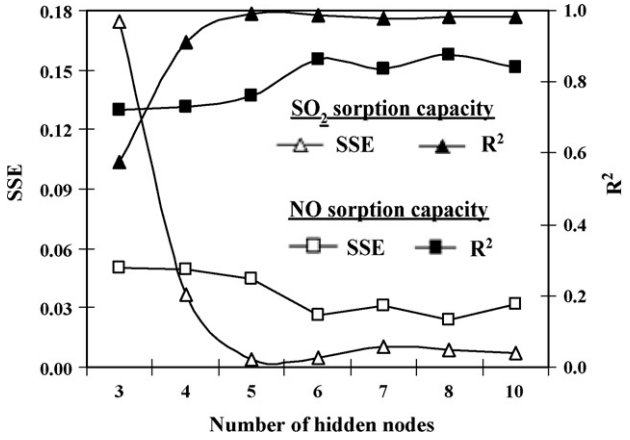

Fig. 1. Selection of optimal number of neurons in the hidden layer resulted from a series of NN topologies.

model was used to predict the SO_2 and NO sorption capacities in the following section.

3.2. Neural network (NN) modeling

The performance of the NNs topology to estimate the training data set was evaluated in term of the SSE (Eq. (2)) and R^2. Fig. 1 shows the effect of number of hidden neurons in the hidden layer on the NN error (SSE) and R^2 of the training data sets. It can be observed that the optimum number of hidden neurons (that give minimum SSE and high R^2 of 0.004 and 0.990, respectively) was obtained using five hidden neurons for SO_2 sorption capacity. For NO sorption capacity, six hidden neurons were observed to give minimum SSE of 0.024 and high R^2 of 0.877. The result also shows that the networks with more than six hidden neurons did not improve the fitting criterions for both SO_2 and NO sorption capacities. Therefore it was decided to use a network with six hidden neurons. Based on the approximation of SSE function and R^2, a NN with 4-6-2 structure was implemented in this study for the prediction of SO_2 and NO sorption capacities.

The testing and validation results for the particular NN model for the prediction of SO_2 and NO sorption capacities (after rescaling) are shown in Fig. 2. It can be observed that most points are nearby the line adjustment which means that the values determined experimentally are similar to those determined by the NN model. The R^2 values for testing and validation of SO_2 sorption capacity (Fig. 2a) were 0.997 and 0.853, respectively. Concurrently, the R^2 values for testing and validation of NO sorption capacity (Fig. 2b) were 0.994 and 0.916, respectively. Although the validation results were found to give lower R^2 values as compared to testing results, however, it still provide an accurate prediction for SO_2 and NO sorption capacities of the RHA/CaO/CeO_2 sorbents within the range of the sorbent preparation variables studied. Moreover, the results in Fig. 2 establish the effectiveness of NNs as a powerful computational tool for modeling small data sets obtained from the experimental results.

3.3. Attaining optimum condition

Based on the results obtained from CCD experiment and NN modeling for RHA/CaO/CeO_2 sorbents, the level of significant variables were further optimized using the point prediction function (or regression model) given by Design Expert software. Other than that, optimization was also carried out to determine whether the use of RHA_{raw} or $RHA_{600°C}$ (in the preparation of RHA/CaO/CeO_2 sorbents) is more favorable in producing sorbent with a higher SO_2/NO sorption capacity. In order to locate the optimum hydration process variable that could produce RHA/CaO/CeO_2 sorbents with the highest SO_2/NO sorption capacity, the variables objective was chosen as follows. Although RHA/CaO ratio (x_2) and type of RHA (x_4) were found not to have significant effect, but both were still included in the optimization procedure as in our previous study, both parameters were found to have significant effect [7,8]. For hydration period (x_1) and CeO_2 loading (x_3), although these two variables have significant effect, however, when it comes to practical application of this technology, the value used for these two variables must always be at the lowest for economical feasibility. Thus in the optimization work, these variables (x_1 and x_3) were chosen at the minimum range. Then, the numerical optimization feature in Design Expert software was used to search for a combination of variables levels that simultaneously satisfy the requirements placed on each of the responses and variables.

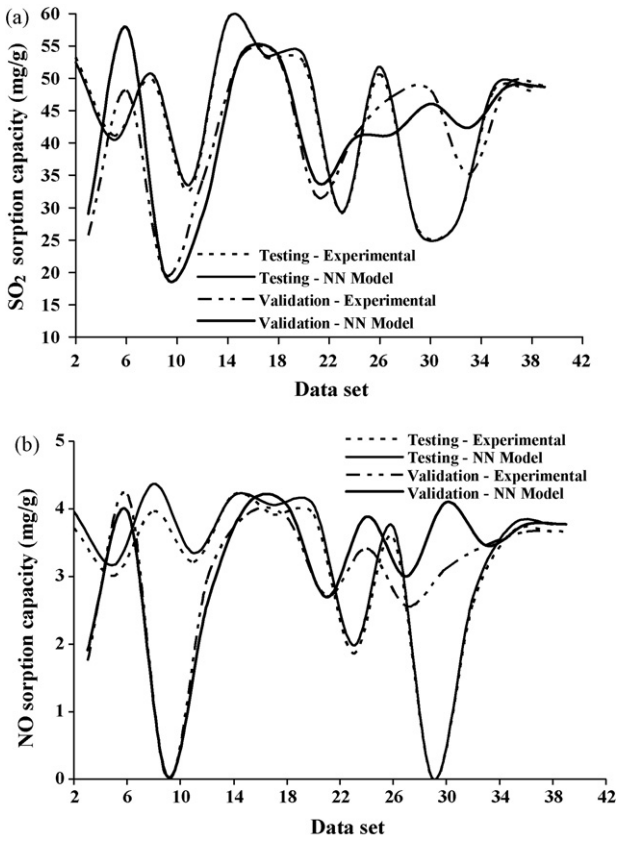

Fig. 2. NN model results for (a) testing and validation of SO_2 sorption, and (b) testing and validation of NO sorption.

Figs. 3 and 4 show the contour plots for predicting maximum SO_2 and NO sorption capacities for RHA/CaO/CeO_2 sorbents prepared from RHA_{raw} and $RHA_{600°C}$, respectively under optimum conditions selected. The RHA/CaO/CeO_2 sorbents prepared from RHA_{raw} and $RHA_{600°C}$ hereinafter are labeled to as sorbent E1 and E2, respectively. It was predicted that a maximum SO_2 and NO sorption capacities of 44.34 and 3.51 mg/g, respectively can be obtained for sorbent E1 within the range of the hydration process variables investigated. The hydration conditions that result in the maximum sorption capacities are hydration period (x_1) of 12 h, RHA/CaO ratio (x_2) of 2.33 and CeO_2 loading (x_3) of 8.95%. However, lower SO_2 and NO sorption capacities of 42.21 and 3.19 mg/g, respectively were obtained if sorbent E2 were prepared from $RHA_{600°C}$ using hydration period (x_1) of 12 h, RHA/CaO ratio (x_2) of 2.15 and CeO_2 loading (x_3) of 8.43%.

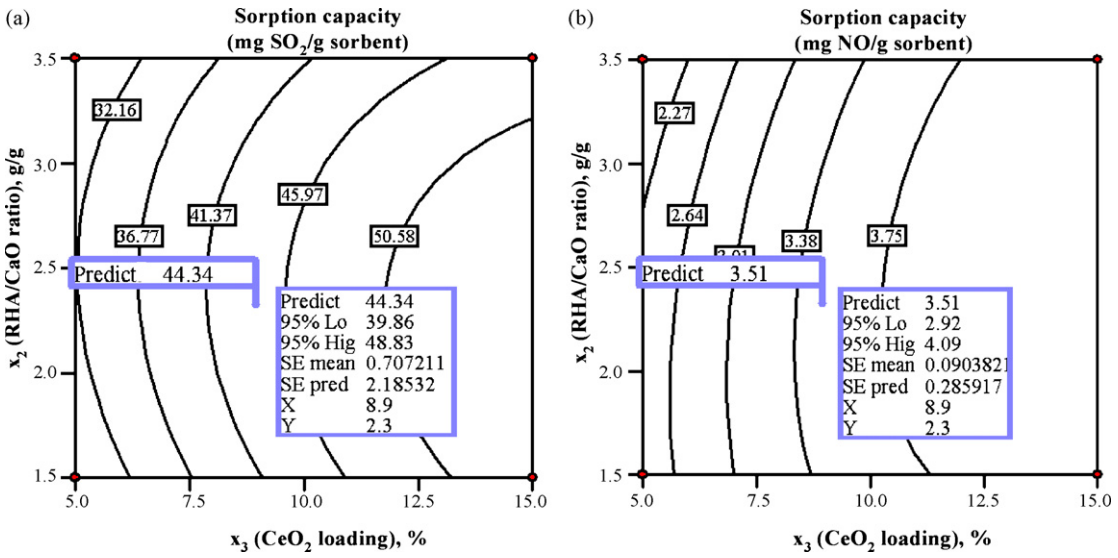

Fig. 3. Contour plot of (a) SO_2 and (b) NO sorption capacities as a function of RHA/CaO ratio and CeO_2 loading for sorbent E1 prepared from RHA_{raw}.

In order to verify the prediction given by CCD (regression) model, sorbents E1 and E2 were prepared under the condition predicted. Three repeated experiments were then carried out for SO_2 and NO sorption test for both sorbents prepared. The results of experiments and the error between the experimental and predicted (by regression model) values are presented in Table 3. The experimental average values of 46.04 mg SO_2/g sorbent and 3.67 mg NO/g sorbent were obtained for sorbent E1. These experimental findings were in close agreement with the model prediction as the error between the experimental and predicted values was found to be 3.84% and 4.45%, respectively for SO_2 and NO sorption capacities. Similarly, the results obtained for sorbent E2 shows that the model developed were also successful in correlating the hydration process variables to SO_2 and NO sorption capacities with a high degree of accuracy.

To further verify the predictive capability of the CCD models, again NN model (with 4-6-2 structure) that has been previously developed was used to predict the maximum SO_2 and NO sorption capacities under optimum hydration process conditions. The previous data sets (Table 1) were used to train the NN model using the backpropagation algorithm (Levenberg–Marquardt method), whereby the two new experimental data sets were incorporated within the validation subsets. In other words, there are two new data sets in the validation subsets, while other data sets (in the training and testing subset) will remain the same. The SO_2 and NO sorption capacities values predicted by NN model is also presented in Table 3. According to NN model, a maximum achievable SO_2 and NO sorption capacities of 47.75 and 3.83 mg/g were obtained for sorbent E1 within the range experimentally investigated. At the same time, NN model also provided predictions of the SO_2 and NO sorption capacities for sorbent E2 very close to those measured experimentally. It is evident that NN predictions gave an excellent agreement with the experimental data as the calculated error between them is less than 5%. This also shows that the NN approach presented in this study can be exploited as an alternative to the conventional quadratic polynomials model for representing data derived from statistically designed experiment.

From the optimization results shown in Table 3, it is obvious that sorbent E1 prepared from RHA_{raw} gives a higher SO_2 and NO sorption capacities compared to sorbent E2 prepared from $RHA_{600^\circ C}$.

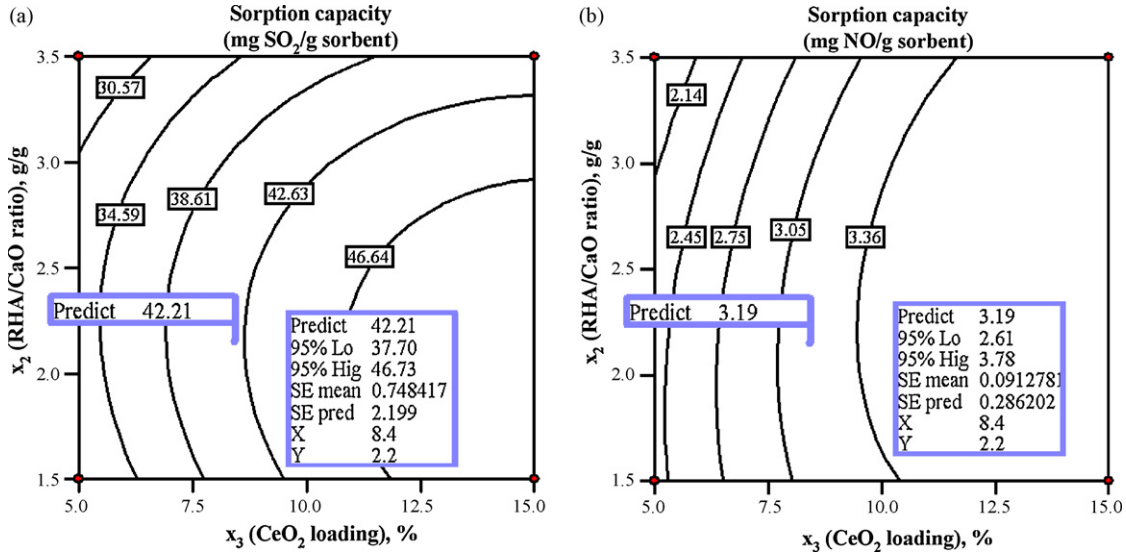

Fig. 4. Contour plot of (a) SO_2 and (b) NO sorption capacities as a function of RHA/CaO ratio and CeO_2 loading for sorbent E2 prepared from $RHA_{600^\circ C}$.

Table 3
Comparison of the optimized results, experimental results and predicted by NN model under optimization criteria for prepared RHA/CaO/CeO_2 sorbents.

RHA-based sorbents	Experimental (mg/g)	Predicted by CCD (mg/g)	Error[a] (%)	Predicted by NN (mg/g)	Error[a] (%)
SO_2 sorption capacity (y_S)					
E1	46.33 45.47 46.33	44.34	3.84	47.75	−3.58
E2	42.90 43.76 43.76	42.21	2.98	44.88	−3.14
NO sorption capacity (y_N)					
E1	3.72 3.62 3.67	3.51	4.45	3.83	−4.34
E2	3.31 3.36 3.36	3.19	4.96	3.47	−3.64

[a] Average value.

These results suggested that apart from CeO_2 (metal oxide) loading, the content of silica also become an important parameter affecting the sorption capacity of the sorbents prepared from RHA. As reported from previous study, the content of silica in the sorbent was closely related to the sorption activity [26,29,34,35] whereby SO_2 and NO sorption capacities markedly increased with the content of silica in the siliceous-calcium-based sorbents. However, in this study sorbents prepared with higher silica content (sorbents E2) displayed contradictory results. This might be due to the phase of the active component (Si–Ca complexes) particularly silica phases in the sorbent that was altered after the calcination process. In the process of synthesizing sorbents E2, the sorbent has been calcined at 600 °C for twice, *i.e.* during the pre-treatment of raw RHA and after impregnation process. As reported from previous researchers [36–38], the silica content in RHA is a thermally sensitive compound. Although it was reported from previous study [8] that heating raw RHA at 600 °C did not change the structure of silica from amorphous to crystalline, however, it is believed that the active component of silica phases in the sorbent E2 has been altered, which then gives low sorption capacities towards SO_2 and NO as compared with sorbent E1.

In order to confirm this presumption, sorbents E1 and E2 were subjected to X-ray diffraction (XRD) analysis. For comparison, sorbents D14 (prepared from RHA_{raw}) and D34 (prepared from $RHA_{600°C}$) from Table 1 (under the same hydration process variables) were also analyzed using XRD. The XRD pattern shown in Fig. 5 illustrated that the diffraction lines of silica ($2\theta \sim 22°$) and calcite ($2\theta \sim 29.4°$) phases on the sorbent E1 and D14 prepared from RHA_{raw} are more pronounced than that of the sorbent E2 and D34 prepared from $RHA_{600°C}$. This result was analogous to previous XRD pattern of RHA/CaO/CeO_2 sorbents prepared from RHA_{raw} although different hydration process variables were applied [10]. In addition, the presence of any unburned carbon content (represented by LOI values) might influence the sorption capacity of SO_2 and NO. Furthermore, this LOI values together with CeO_2 loading and the altered silica phases in the RHA might also lead to alter the physical properties of the RHA-based sorbent. Table 4 lists the physical properties of the selected RHA/CaO/CeO_2 sorbents. It was revealed

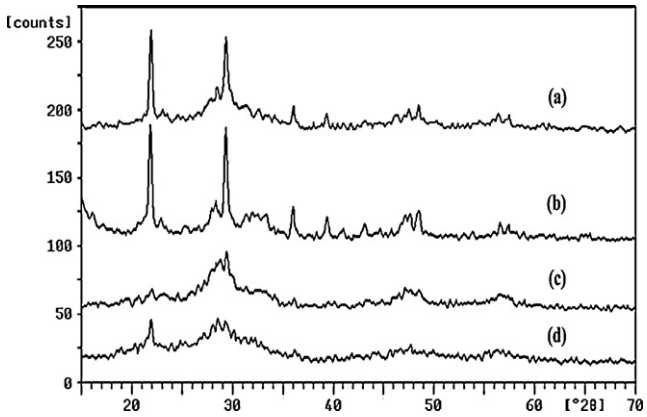

Fig. 5. XRD spectrum of (a) sorbent E1, (b) sorbent D14, (c) sorbent E2 and (d) sorbent D34.

that the surface area of the sorbent E1 and D14 were slightly lower than sorbent E2 and D34. Nevertheless, the total pore volume of the sorbent E1 and D14 shows increment, which is a direct indication that there is an increase in the porosity of the sorbent. With a higher porosity, SO_2 and NO molecules could penetrate easier within the sorbent to react and form mainly sulfate and nitrate products [10]. Furthermore, the reaction between SO_2/NO and the RHA/CaO/CeO_2 sorbent take place mainly in the mesopore region and this has been widely reported for sorbent prepared from siliceous/calcium-based materials.

3.4. Comparison of various sorbents sorption capacities

The activity of the optimized sorbents prepared in this study was compared with other sorbents made from other siliceous materials that have been reported in the literature. Table 5 presents the comparison of various sorbents sorption capacity. It was shown that various raw materials had very low sorption capacity as they could only achieve sorption capacities below 5 mg SO_2/g sorbent

Table 4
Physical properties of RHA/CaO/CeO_2 sorbents.

RHA-based sorbents	BET specific surface area (m^2/g)	Total pore volume (cm^3/g)	Average pore diameter (nm)
Sorbent E1	89.16	0.29	11.02
Sorbent D14	84.23	0.32	9.89
Sorbent E2	95.87	0.15	16.75
Sorbent D34	92.54	0.17	13.16

Table 5
Comparison of the sorption capacity of various sorbents with its base materials during 100% removal.

Sorbents	BET surface area (m^2/g)	SO_2 sorption (mg/g)	NO sorption (mg/g)	Reference
Coal fly ash	1.46	0.21	–	[39]
Oil palm ash	10.2	0.15	–	[40]
Rice husk ash (RHA)	56.31	1.72	–	Present study
CaO	8.66	4.29	–	Present study
Coal fly ash/$Ca(OH)_2$	21.5	18.9[a]	–	[41]
Coal fly ash/CaO/$CaSO_4$	64.5	6.43[b]	–	[39]
Oil palm ash/$Ca(OH)_2$/$CaSO_4$	88.3	2.14[b]	–	[40]
Oil palm ash/$Ca(OH)_2$/$CaSO_4$	127.7[c]	7.35[b]	–	[42]
RHA/CaO	109.39	17.16[a]	–	[7]
RHA/CaO/NaOH	–	19.73[b]	–	[8]
RHA/CaO/CeO_2 (E1)	89.16	46.04[b,c]	3.67[b,c]	Present study

[a] Sorption capacity at highest value.
[b] Sorption capacity at optimum condition.
[c] Average value.

and were unable to remove NO. Conversely, sorbent synthesized from RHA was far superior than the other sorbents. In particular, the RHA/CaO/CeO_2 sorbents prepared in this study exhibited very high sorption capacity and moreover, it could remove SO_2 and NO simultaneously.

4. Conclusions

The parameters optimization for predicting SO_2/NO sorption capacity of RHA/CaO/CeO_2 sorbent is successfully carried out with response surface and artificial neural network models. The second-order response surface models were adequate to predict the SO_2 and NO sorption capacities within four independent sorbent preparation variables. The prediction of these models was verified by neural network models. Response surface models and neural network models were effectively used to find and validate the optimum conditions of the hydration process variables for maximizing the SO_2 and NO sorption capacities.

Acknowledgements

The authors wish to acknowledge the financial support from the Ministry of Science, Technology and Innovation (MOSTI) Malaysia, Yayasan Felda and Universiti Sains Malaysia (Short Term Grant A/C. 6035278 and RU Golden Goose Project Grant A/C. 814004).

References

[1] N. de Nevers, Air Pollution Control Engineering, 2nd ed., McGraw-Hill, Whitehouse Station, 2000.
[2] R.F. Probstein, R.E. Hicks, Synthetic Fuel, Dover Publications, New York, 2006.
[3] J.L. Zhu, Y.H. Wang, J.C. Zhang, R.Y. Ma, Experimental investigation of adsorption of NO and SO_2 on modified activated carbon sorbent from flue gases, Energ. Convers. Manage. 46 (2005) 2173–2184.
[4] Bronzeoak Ltd., Available from World Wide Web: http://www.dti.gov.uk/energy/renewables/publications/pdfs/exp129.pdf.
[5] Food and Agriculture Organization of the United Nations, Available from World Wide Web: http://faostat.fao.org/site/567/DesktopDefault.aspx?%20PageID=567# ancor.
[6] K.T. Lee, A.M. Mohtar, N.F. Zainudin, S. Bhatia, A.R. Mohamed, Optimum conditions for preparation of flue gas desulfurization absorbent from rice husk ash, Fuel 84 (2005) 143–151.
[7] I. Dahlan, K.T. Lee, A.H. Kamaruddin, A.R. Mohamed, Key factor in rice husk ash/CaO sorbent for high flue gas desulfurization activity, Environ. Sci. Technol. 40 (2006) 6032–6037.
[8] I. Dahlan, K.T. Lee, A.H. Kamaruddin, A.R. Mohamed, Analysis of SO_2 sorption capacity of rice husk ash (RHA)/CaO/NaOH sorbents using response surface methodology (RSM): un-treated and pre-treated RHA, Environ. Sci. Technol. 42 (2008) 1499–1504.
[9] I. Dahlan, K.T. Lee, A.H. Kamaruddin, A.R. Mohamed, Evaluation of various additives on the preparation of rice husk ash (RHA)/CaO-based sorbent for flue gas desulfurization (FGD) at low temperature, J. Hazard. Mater. 161 (2009) 570–574.
[10] I. Dahlan, K.T. Lee, A.H. Kamaruddin, A.R. Mohamed, Selection of metal oxides in the preparation of rice husk ash (RHA)/CaO sorbent for simultaneous SO_2 and NO removal, J. Hazard. Mater. 166 (2009) 1556–1559.
[11] K.D. Deeng, A.R. Mohamed, S. Bhatia, Process optimization studies of structured Cu-ZSM-5 zeolite catalyst for the removal of NO using design of experiments (DOE), Chem. Eng. J. 103 (2004) 147–157.
[12] K.T. Lee, S. Bhatia, A.R. Mohamed, K.H. Chu, Optimizing the specific surface area of fly ash-based sorbents for flue gas desulfurization, Chemosphere 62 (2006) 89–96.
[13] K.T. Lee, S. Bhatia, A.R. Mohamed, Optimization of process parameters for the preparation of CaO/$CaSO_4$/coal fly ash sorbent for sulfur dioxide (SO_2) removal: part II, Energ. Sources Part A 28 (2006) 1251–1258.
[14] I.A.W. Tan, A.L. Ahmad, B.H. Hameed, Optimization of preparation conditions for activated carbons from coconut husk using response surface methodology, Chem. Eng. J. 137 (2008) 462–470.
[15] D. Bas, I.H. Boyaci, Modeling and optimization II: comparison of estimation capabilities of response surface methodology with artificial neural networks in a biochemical reaction, J. Food Eng. 78 (2007) 846–854.
[16] J. Huang, L.H. Mei, J. Xia, Application of artificial neural network coupling particle swarm optimization algorithm to biocatalytic production of GABA, Biotechnol. Bioeng. 96 (2007) 924–931.
[17] A. Aleboyeh, M.B. Kasiri, M.E. Olya, H. Aleboyeh, Prediction of azo dye decolorization by UV/H2O2 using artificial neural networks, Dyes Pigment. 77 (2008) 288–294.
[18] L. He, Y.-Q. Xu, X.-H. Zhang, Medium factor optimization and fermentation kinetics for phenazine-1-carboxylic acid production by pseudomonas sp. M18G, Biotechnol. Bioeng. 100 (2008) 250–259.
[19] A.B. Chelani, C.V.C. Rao, K.M. Phadke, M.Z. Hasan, Prediction of sulphur dioxide concentration using artificial neural networks, Environ. Model. Softw. 17 (2002) 161–168.
[20] A.L. Ahmad, I.A. Azid, A.R. Yusof, K.N. Seetharamu, Emission control in palm oil mills using artificial neural network and genetic algorithm, Comput. Chem. Eng. 28 (2004) 2709–2715.
[21] G. Nunnari, S. Dorling, U. Schlink, G. Cawley, R. Foxall, T. Chatterton, Modelling SO_2 concentration at a point with statistical approaches, Environ. Model. Softw. 19 (2004) 887–905.
[22] R.O.E. Hooi, K.T. Lee, A.R. Mohamed, K.H. Chu, Neural network modeling of the kinetics of SO2 removal by fly ash-based sorbent, J. Environ. Sci. Health Part A-Toxic/Hazard. Subst. Environ. Eng. 41 (2006) 195–210.
[23] A. Tholudur, W.F. Ramirez, Neural-network modeling and optimization of induced foreign protein production, AIChE J. 45 (1999) 1660–1670.
[24] K. Huang, F.-Q. Chen, D.-W. Lu, Artificial neural network-aided design of a multicomponent catalyst for methane oxidative coupling, Appl. Catal. A-Gen. 219 (2001) 61–68.
[25] Z. Ahmad, J. Zhang, Selective combination of multiple neural networks for improving model prediction in nonlinear systems modeling through forward selection and backward elimination, Neurocomputing 72 (2009) 1198–1204.
[26] R.-B. Lin, S.-M. Shih, C.-F. Liu, Characteristics and reactivities of $Ca(OH)_2$/silica fume sorbents for low-temperature flue gas desulfurization, Chem. Eng. Sci. 58 (2003) 3659–3668.
[27] H.-H. Tseng, M.-Y. Wey, Y.-S. Liang, K.-H. Chen, Catalytic removal of SO_2, NO and HCl from incineration flue gas over activated carbon-supported metal oxides, Carbon 41 (2003) 1079–1085.
[28] D.C. Montgomery, Design and Analysis of Experiments, 5th ed., John Wiley & Sons, New York, 2001.
[29] J.R. Peterson, G.T. Rochelle, Aqueous reaction of fly ash and $Ca(OH)_2$ to produce calcium silicate absorbent for flue gas desulfurization, Environ. Sci. Technol. 22 (1988) 1299–1304.
[30] A. Garea, I. Fernandez, J.R. Viguri, M.I. Ortiz, J. Fernandez, M. Renedo, J.A. Irabien, Fly-ash/calcium hydroxide mixtures for SO_2 removal: Structural properties and maximum yield, Chem. Eng. J. 66 (1997) 171–179.
[31] X. Zheng, S. Wang, S. Wang, S. Zhang, W. Huang, S. Wu, Copper oxide catalysts supported on ceria for low-temperature CO oxidation, Catal. Commun. 5 (2004) 729–732.
[32] L. Fen, Y. Bo, Z. Jie, J. Anxi, S. Chunhong, K. Xiangji, W. Xin, Study on desulfurization efficiency and products of Ce-doped nanosized ZnO desulfurizer at ambient temperature, J. Rare Earths 25 (2007) 306–310.

[33] A. Trovarelli, C. de Leitenburg, M. Boaro, G. Dolcetti, The utilization of ceria in industrial catalysis, Catal. Today 50 (1999) 353–367.
[34] W. Jozewicz, G.T. Rochelle, Fly ash recycle in dry scrubbing, Environ. Prog. 5 (1986) 218–223.
[35] H. Tsuchiai, T. Ishizuka, H. Nakamura, T. Ueno, H. Hattori, Study of flue gas desulfurization absorbent prepared from coal fly ash: Effects of the composition of the absorbent on the activity, Ind. Eng. Chem. Res. 35 (1996) 2322–2326.
[36] A. Proctor, X-ray diffraction and scanning electron microscope studies of processed rice hull silica, J. Am. Oil Chem. Soc. 67 (1990) 576–584.
[37] N. Yalcin, V. Sevinc, Studies on silica obtained from rice husk, Ceram. Int. 27 (2001) 219–224.
[38] V.P. Della, I. Kuhn, D. Hotza, Rice husk ash as an alternate source for active silica production, Mater. Lett. 57 (2002) 818–821.
[39] K.T. Lee, Flue gas desulfurization studies using absorbent prepared from coal fly ash, Ph.D. thesis, Universiti Sains, Malaysia, 2004.
[40] N.F. Zainudin, Utilization of oil palm ash (OPA) as an absorbent for the removal of sulfur dioxide (SO_2) from flue gas, M.Sc. thesis, Universiti Sains, Malaysia, 2005.
[41] J.C. Martinez, J.F. Izquierdo, F. Cunill, J. Tejero, J. Querol, Reactivation of fly ash and $Ca(OH)_2$ mixtures for SO_2 removal of flue gas, Ind. Eng. Chem. Res. 30 (1991) 2143–2147.
[42] A.R. Mohamed, K.T. Lee, N.M. Noor, N.F. Zainudin, Oil palm ash/CaO/$CaSO_4$ absorbent for flue gas desulfurization, Chem. Eng. Technol. 28 (2005) 939–945.